



Prospects for the Use of Carbon-based Perovskite Solar Cells



Vladislav A. Kinev¹, Pavel P. Gladyshev^{1*} and Medhat A. Ibrahim²

¹Dubna State University, 19 University Str., Dubna, 141980, Moscow region, Russian Federation.

²Spectroscopy Department, National Research Center, 33 El-Bohouth Str., 12622 Dokki, Giza, Egypt.

FOR the first time, perovskite solar cells were demonstrated in 2009, and since then have been the subject of intense study. Due to the fact that perovskite has a band gap zone with direct transitions, it absorbs light more efficiently than silicon, and a thin layer is required to produce a solar cell, which can be obtained by precipitation from solution, which significantly reduces the cost of production of perovskite solar cells. Recently organic-inorganic hybrid lead-halide perovskite solar cells (PSCs) achieved a certified energy conversion efficiency of 23.7%. Among the various types of PSCs, carbon-based hole-conductor-free perovskite solar cells (CPSGs) were gradually recognized as the most promising for the commercialization with the advantages of low cost, high stability and easy fabrication. Here we review the latest developments in the field of printable carbon-based hole-conductor-free perovskite solar cells.

Keywords: Perovskite solar cells, Hole-conductor-free, Carbon materials.

Introduction

Semiconductor photoelectric converters are the most efficient devices for converting solar radiation energy into electrical energy. The exceptional photovoltaic properties demonstrated for organic-inorganic hybrid lead-halide perovskites (for example, $\text{CH}_3\text{NH}_3\text{PbX}_3$, X = Cl, Br, I) attracted immense attention from scientists all over the world [1-6]. Intriguing optoelectronic characteristics include broad spectral absorption, low exciton binding energy, high charge carrier mobility and a significant diffusion length of charges [7-11]. Organic-inorganic hybrid lead-halide perovskite solar cells (PSCs) rapidly appeared on the leading edge of photovoltaic technologies with a certified power conversion rate of 23.7% [12].

A TiO_2 / perovskite/ HTM/ Au device configuration is commonly used in typical PSC. Spiro-OMeTAD or PTAA (poly(triaryl)amine) are the most common choice for hole transport materials (HTM) [13-15]. However, the high cost

of spiro-OMeTAD or PTAA and their instability under the influence of atmospheric air becomes a serious problem for the development of PSCs [16-18]. Fortunately, perovskite material (such as $\text{CH}_3\text{NH}_3\text{PbX}_3$) has a high mobility of charge carriers and can serve as the hole carrier itself, which makes it unnecessary to use additional material to transport them [19-23]. However, the absence of HTM layer causes a decrease in the efficiency of the PSCs, because the HTM not only transfers holes, but also blocks electrons, preventing the recombination of charges, which is a very important point.

HTM-free perovskite solar cells mainly include Au-based or carbon-based PSC [19,21,24-27]. However, Au is too expensive for mass industrial manufacture. Evaporating Au or Ag onto the top of the cell is a high energy-consumption process which needs high vacuum and high temperature, thereby limiting its commercial use [28-31].

To create simple and inexpensive photovoltaic device there were developed carbon-based PSCs not containing HTM [20,21,23,32-36]. Carbon

*Corresponding author e-mail: pglad@yandex.ru

Received 28/2/2019; Accepted 21/5/2019

DOI: 10.21608/ejchem.2019.12753.1793

©2019 National Information and Documentation Center (NIDOC)

materials, especially graphite, carbon black and carbon nanotubes, have such characteristics as low cost, high electrical conductivity, accessibility, controlled porosity, chemical stability and environmental friendliness [37]. Taking these advantages, carbon is considered the most promising for electrode materials [22, 38]. In 2013, the Han group firstly reported about carbon-containing mesoscopic perovskite solar cells (m-CPSCs) without HTM [20]. Mesoscopic three-layer frame can be made by simple and cheap screen-printing technology, which offers a more positive perspective for commercial production [38]. In addition, they used $(HOOC(CH_2)_4NH_3)_x(CH_3NH_3)_{1-x}PbI_3$ (hereinafter $(5\text{-AVA})_x(MA)_{1-x}PbI_3$) as a light absorber in the form of m-CPSCs and achieved a certified efficiency of 12.84% which was stable for more than 1000 hours without encapsulation in atmospheric air under the influence of light AM 1,5 G [21]. Recently, they manufactured a large-sized ($10 \times 10 \text{ cm}^2$) printed mesoscopic perovskite solar module with an efficiency exceeding 10%. It is stable in local environmental conditions for 1 month and resistant to storage for more than one year [39]. Thus, the excellent characteristics of carbon-based m-CPSCs without the use of HTM make it one of the most promising solar cells for commercialization.

Device architecture and working principle

Carbon-based PSCs without HTM can be divided into two categories based on different types of carbon electrodes, such as a mesoscopic carbon electrode and a flat carbon electrode. As shown in Fig. 1a, typical HTM-free mesoscopic carbon-based PSCs (m-CPSCs) have a triple mesoscopic layer comprising TiO_2 , ZrO_2 and carbon, acting as an electron transport layer, separation layer and hole collection layer, respectively. Triple layer is screen printed on FTO substrate layer by layer, followed by sintering. Then the perovskite precursor solution is infiltrated into the mesoscopic framework by drop-casting precursor solution from the carbon side. Perovskite crystals are formed after annealing. The schematic structure of a planar HTM-free carbon-based PSCs (p-CPSCs) consists of FTO/ TiO_2 /perovskite/ carbon, as shown in Fig. 1b. Unlike m-CPSCs, p-CPSCs are manufactured in the same way as conventional PSCs using an Au electrode. Layers of m- TiO_2 and perovskite are deposited by spin coating on a thin planar layer of TiO_2 deposited on FTO, and then the layer of carbon is deposited on the surface of the perovskite layer [23,35,40].

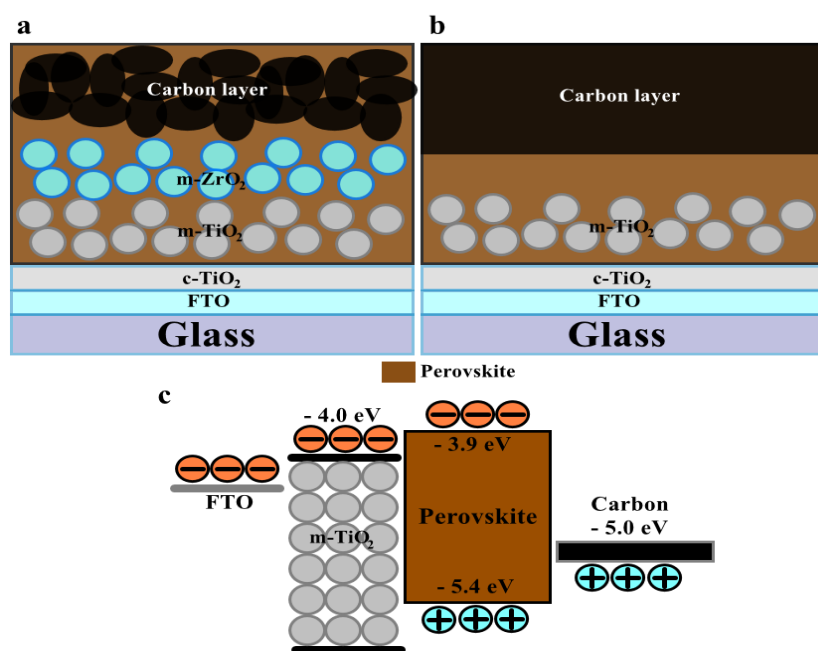


Fig.1.Schematic illustration of the structure of devices (a) m-CPSCs and (b)p-CPSCs.
(c) Energy band diagram of CPSCs device.

The alignment of energy levels for three functional layers in the CPSCs device is presented in Fig. 1c. The conduction band edge (-3.9 eV) of perovskite MAPbI_3 is higher than the conduction band edge (-4.0 eV) of TiO_2 , and the edge of the valence band (-5.4 eV) is lower than the Fermi level (-5.0 eV) of carbon. Electrons and holes are generating in the conduction band and the valence band of MAPbI_3 after absorption of light radiation by the perovskite absorber. Then the photogenerated electrons move to the conduction band of TiO_2 , the holes are extracted by carbon. Spacer layer, such as m-ZrO_2 , is commonly used in m-PSCs without HTM to separate the TiO_2 and carbon layer. Due to the absence of the HTM layer, direct contact of the TiO_2 and the carbon layer can lead to a short circuit and then seriously affect the operation of the device. However, the separation layer is not needed for p-CPSCs without HTM, a thick layer of perovskite material on the surface of TiO_2 usually strongly separates TiO_2 and carbon.

Carbon-based HTM-free Perovskite solar modules

It is necessary to manufacture large-sized perovskite solar modules (PSM) for commercialization of PSCs. Recently, Hu et al. [39] have successfully achieved new results, when they created PSM systems without HTM with sizes up

to 100 cm^2 using cost-effective screen-printing technology (Fig. 2). Carbon-based perovskite solar modules (CPSM) ($10 \times 10 \text{ cm}^2$) are consisted of 10 series-connected cells showing an efficiency of 10.4% in the active area of 49 cm^2 (Fig. 3). PSM showed good stability without encapsulation during continuous illumination for 1000 hours in ambient conditions with a temperature of 25°C and humidity (RH) of 54%. The surface temperature of the device reached 50°C and were stabilized throughout the test under continuous illumination. They also tested the external stability of encapsulated devices for 1 month in a local environment with an average temperature of around 30°C and an RH of 80% in Wuhan, China, and no deteriorations was observed. In addition, they made a fully printable 7 m^2 perovskite solar panel, demonstrating good reproducibility of screen-printing technology in the manufacture of high-performance PSM. This paved the way for the implementation of an efficient and stable large area PSM for industrial deployment. At the same time, the Subodh group also produced a 70 cm^2 PSM on the basis of the exact same structure, which shows stability in the environment for more than 2000 hours with a decrease in efficiency less than 5% [41]. The main achievements of the study of PSCs without HTM are represented in Table 1.

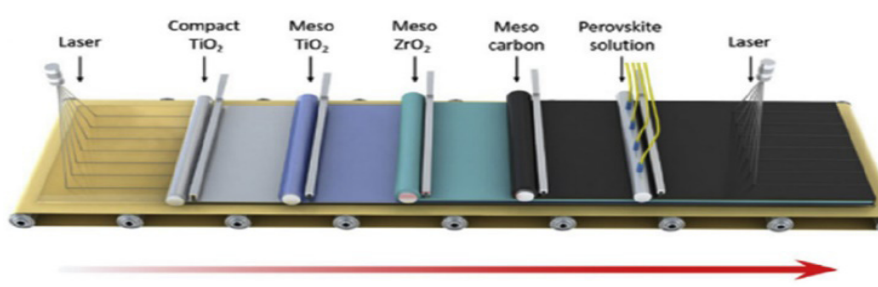


Fig. 2. Schematic illustration of the proposed production line of PSM.[39].

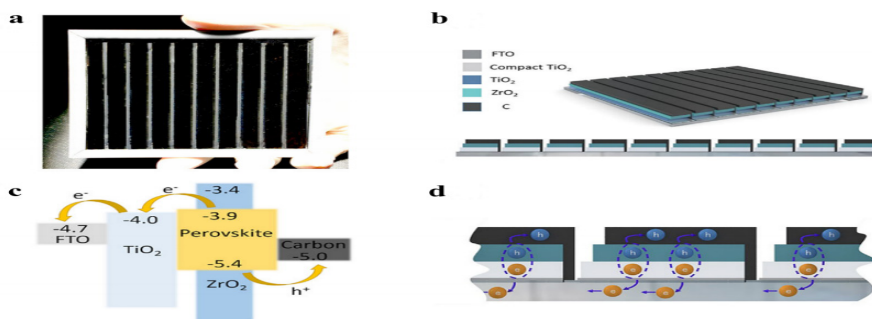


Fig. 3. (a) Image of a monolithic printable PSM with 10 subcells. (b) The monolithic interconnection scheme of the module. [39]

TABLE 1. Main devices of CPSC type without HTM and indications of their effectiveness.

Device structure	PCE (%)	Ref.
FTO/(TiO ₂ /ZrO ₂ /carbon)/MAPbI ₃	6,64	[20]
FTO/(TiO ₂ /ZrO ₂ /carbon)/MAPbI ₃	12,84	[21]
FTO/(TiO ₂ /ZrO ₂ /carbon)/MAPbI ₃	13,89	[44]
FTO/(TiO ₂ /ZrO ₂ /carbon)/MAPbI ₃	14,50	[43]
FTO/(TiO ₂ /ZrO ₂ /carbon)/MAPbI ₃	15,60	[42]
FTO/TiO ₂ /MAPbI ₃ /carbon	8,31	[36]
FTO/TiO ₂ /MAPbI ₃ /carbon	9,08	[30]
FTO/TiO ₂ /MAPbI ₃ /carbon	13,53	[35]
FTO/TiO ₂ /MAPbI ₃ /carbon	14,38	[45]
FTO/TiO ₂ /MAPbI ₃ /CNTs	6,29	[48]
FTO/TiO ₂ /MAPbI ₃ /MCWNTs	12,67	[49]
FTO/TiO ₂ /Al ₂ O ₃ /MAPbI ₃ /MCWNTs	15,23	[52]
FTO/(ZnO/TiO ₂ /ZrO ₂ /carbon)/MAPbI ₃	8,24	[50]
FTO/TiO ₂ /SiO ₂ /MAPbI ₃ /carbon	11,90	[51]
FTO/TiO ₂ /CsPbBr ₃ /carbon	6,70	[47]
FTO/TiO ₂ /(FA) _x (MA) _{1-x} PbI ₃ /carbon	13,03	[46]

Molecular modeling approaches

Molecular modeling with different level of theories is applying the basis of physics to understand chemical structures and materials functionality [53].

Molecular modeling offers tools for investigating chemical structure in which experimental setup is limited and/or unavailable [54-55]. It's now an effective tool to elucidate the functionality of emerging and new materials based on their electronic properties [56-60]. The structural properties, the efficiency of absorption and reflection of the solar cell made of perovskites could be investigated with molecular modeling at density functional theory DFT level of theory [61-63]. It is stated that, combining both DFT and finite difference time domain (FDTD) method could an effective tool of computation to assess the different properties of solar cell made of perovskites [64]. It is also stated that, relativistic GW approximation has been demonstrated to provide electronic structure accurately with extremely high computational cost [65-68]. Attempts were carried out by many researchers to predict the properties of newly designed perovskites with accurate at a low computational cost [69]. An exchange-correlation functional

based on DFT is utilized to predict the band gap in organic-inorganic metal halide perovskites [70].

It could be concluded in this section that DFT as well as modified DFT level of theories are dedicated now to investigate and/or innovate new features for perovskite solar cells. This findings is in good agreement of the previous findings [71-73].

Conclusion and outlook

In this paper we focused on recent advances of low-cost carbon-based hole-conductor-free perovskite solar cells in terms of perovskite solar cell modifications and large surface perovskite solar modules. Carbon-based PSCs without HTM demonstrate high stability during continuous illumination in environmental conditions, which makes them one of the most promising solar cells for commercialization. However, the current efficiency for HTM-free CPSCs is still lower than that of conventional PSCs based on HTM. Therefore, improving the efficiency of devices is a major priority.

The mechanism of excellent stability of HTM-free CPSCs has not been fully studied. Further work should focus on studying of the relation between stability of the device properties and the peculiarities of its internal architecture, as well as

on the establishment of the aging mechanism of various PSCs components.

References

1. Shi Z., Jayatissa A.; Perovskites-based solar cells: A review of recent progress, materials and processing methods, *Materials*, **11** (5), 729 (2018).
2. Im J.-H., Lee C.-R., Lee J.-W., Park S.-W., Park N.-G.; 6.5% efficient perovskite quantum-dot-sensitized solar cell, *Nanoscale*, **3**, 4088-4093 (2011).
3. Ahn N., Son D.-Y., Jang I.-H., Kang S.M., Choi M., Park N.-G.; Highly reproducible perovskite solar cells with average efficiency of 18.3% and best efficiency of 19.7% fabricated via Lewis base adduct of lead (II) iodide, *J. Am. Chem. Soc.*, **137**, 8696-8699 (2015).
4. Jeon N.J., Noh J.H., Yang W.S., Kim Y.C., Ryu S., Seo J., Seok S.I.; Compositional engineering of perovskite materials for high-performance solar cells, *Nature*, **517**, 476-480 (2015).
5. Li X., Bi D., Yi C., D_ecopet J.-D., Luo J., Zakeeruddin S.M., Hagfeldt A., Gratzel M.; A vacuum flash-assisted solution process for high-efficiency largearea perovskite solar cells, *Science*, **353**, 58-62 (2016).
6. McMeekin D.P., Sadoughi G., Rehman W., Eperon G.E., Saliba M., Horantner M.T., Haghimirad A., Sakai N., Korte L., Rech B., Johnston M.B., Herz L.M., Snaith H.J.; A mixed-cation lead mixed-halide perovskite absorber for tandem solar cells, *Science*, **351**, 151-155 (2016).
7. Stranks S.D., Eperon G.E., Grancini G., Menelaou C., Alcocer M.J., Leijtens T., Herz L.M., Petrozza A., Snaith H.J.; Electron-hole diffusion lengths exceeding 1 micrometer in an organometal trihalide perovskite absorber, *Science*, **342**, 341-344 (2013).
8. Pazos-Outon L.M., Szumilo M., Lamboll R., Richter J.M., Crespo-Quesada M., Abdi-Jalebi M., Beeson H.J., Vrucinic M., Alsari M., Snaith H.J., Ehrler B., Friend R.H., Deschler F.; Photon recycling in lead iodide perovskite solar cells, *Science*, **351**, 1430-1433 (2016).
9. Blancon J.-C., Tsai H., Nie W., Stoumpos C., Pedesseau L., Katan C., Kepenekian M., Soe C., Appavoo K., Sfeir M.; Extremely efficient internal exciton dissociation through edge states in layered 2D perovskites, *Science*, **355**, 1288-1291 (2017).
10. Guo Z., Wan Y., Yang M., Snaider J., Zhu K., Huang L.; Long-range hot-carrier transport in hybrid perovskites visualized by ultrafast microscopy, *Science*, **356**, 59-62 (2017).
11. Xing G., Mathews N., Sun S., Lim S.S., Lam Y.M., Gratzel M., Mhaisalkar S., Sum T.C.; Long-range balanced electron-and hole-transport lengths in organic-inorganic $\text{CH}_3\text{NH}_3\text{PbI}_3$, *Science*, **342**, 344-347 (2013).
12. <https://www.nrel.gov/pv/assets/pdfs/pv-efficiency-chart.20190103.pdf>
13. Gratzel M.; The light and shade of perovskite solar cells, *Nat. Mater.*, **13**, 838-842 (2014).
14. Burschka J., Pellet N., Moon S.-J., Humphry-Baker R., Gao P., Nazeeruddin M.K., Gratzel M.; Sequential deposition as a route to high-performance perovskite-sensitized solar cells, *Nature*, **499**, 316-319 (2013).
15. Gratzel M.; The rise of highly efficient and stable perovskite solar cells, *Acc. Chem. Res.*, **50**, 487-491 (2017).
16. Leijtens T., Eperon G.E., Pathak S., Abate A., Lee M.M., Snaith H.J.; Overcoming ultraviolet light instability of sensitized TiO_2 with meso-superstructured organometal tri-halide perovskite solar cells, *Nat. Commun.*, **4**, 2885 (2013).
17. Berhe T.A., Su W.N., Chen C.H., Pan C.J., Cheng J.H., Chen H.M., Tsai M.C., Chen L.Y., Dubale A.A., Hwang B.J.; Organometal halide perovskite solar cells: degradation and stability, *Energy Environ. Sci.*, **9**, 323-356 (2016).
18. Docampo P., Bein T.; A long-term view on perovskite optoelectronics, *Acc. Chem. Res.*, **49**, 339-346 (2016).
19. Etgar L., Gao P., Xue Z., Peng Q., Chandiran A.K., Liu B., Nazeeruddin M.K., Gratzel M.; Mesoscopic $\text{CH}_3\text{NH}_3\text{PbI}_3/\text{TiO}_2$ heterojunction solar cells, *J. Am. Chem. Soc.*, **134**, 17396-17399 (2012).
20. Ku Z., Rong Y., Xu M., Liu T., Han H.; Full printable processed mesoscopic $\text{CH}_3\text{NH}_3\text{PbI}_3/\text{TiO}_2$ heterojunction solar cells with carbon counter electrode, *Sci. Rep.*, **3** (2013).
21. Mei A., Li X., Liu L., Ku Z., Liu T., Rong Y., Xu M., Hu M., Chen J., Yang Y., Gratzel M., Han H.; A hole-conductor free, fully printable mesoscopic perovskite solar cell with high stability, *Science*, **345**, 295-298 (2014).

22. Chen H., Yang S.; Carbon-based perovskite solar cells without hole transport materials: the front runner to the market? *Adv. Mater.*, **29** (2017).
23. Wei Z., Chen H., Yan K., Yang S.; Inkjet printing and instant chemical transformation of a $\text{CH}_3\text{NH}_3\text{PbI}_3$ /nanocarbon electrode and interface for planar perovskite solar cells, *Angew. Chem.*, **126**, 13455-13459 (2014).
24. Etgar L.; Hole Conductor Free Perovskite-based Solar Cells, *Springer* (2016).
25. Laban W.A., Etgar L.; Depleted hole conductor-free lead halide iodide heterojunction solar cells, *Energy Environ. Sci.*, **6**, 3249-3253 (2013).
26. Shi J., Dong J., Lv S., Xu Y., Zhu L., Xiao J., Xu X., Wu H., Li D., Luo Y.; Holeconductor-free perovskite organic lead iodide heterojunction thin-film solar cells: high efficiency and junction property, *Appl. Phys. Lett.*, **104**, 063901 (2014).
27. Xiao Y., Han G., Chang Y., Zhang Y., Li Y., Li M.; Investigation of perovskite sensitized nanoporous titanium dioxide photoanodes with different thicknesses in perovskite solar cells, *J. Power Sources*, **286**, 118-123 (2015).
28. Zhou H., Shi Y., Dong Q., Zhang H., Xing Y., Wang K., Du Y., Ma T.; Holeconductor-free, metal-electrode-free $\text{TiO}_2/\text{CH}_3\text{NH}_3\text{PbI}_3$ heterojunction solar cells based on a low-temperature carbon electrode, *J. Phys. Chem. Lett.*, **5**, 3241-3246 (2014).
29. Domanski K., Correa-Baena J.-P., Mine N., Nazeeruddin M.K., Abate A., Saliba M., Tress W., Hagfeldt A., Gratzel M.; Not all that glitters is gold: metalmigration-induced degradation in perovskite solar cells, *ACS Nano*, **10**, 6306-6314 (2016).
30. Guerrero A., You J., Aranda C., Kang Y.S., Garcia-Belmonte G., Zhou H., Bisquert J., Yang Y.; Interfacial degradation of planar lead halide perovskite solar cells, *ACS Nano*, **10**, 218-224 (2015).
31. Verdingovas V., Müller L., Jellesen M.S., Grumsen F.B., Ambat R.; Effect of iodine on the corrosion of Au-Al wire bonds, *Corros. Sci.*, **97**, 161-171 (2015).
32. Gholipour S., Correa-Baena J.P., Domanski K., Matsui T., Steier L., Giordano F., Tajabadi F., Tress W., Saliba M., Abate A.; Highly efficient and stable perovskite solar cells based on a low-cost carbon cloth, *Adv. Energy Mater.*, **6** (2016).
33. Chen H., Wei Z., Zheng X., Yang S.; A scalable electrodeposition route to the low-cost, versatile and controllable fabrication of perovskite solar cells, *Nano Energy*, **15**, 216-226 (2015).
34. Ito S., Mizuta G., Kanaya S., Kanda H., Nishina T., Nakashima S., Fujisawa H., Shimizu M., Haruyama Y., Nishino H.; Light stability tests of $\text{CH}_3\text{NH}_3\text{PbI}_3$ perovskite solar cells using porous carbon counter electrodes, *Phys. Chem. Chem. Phys.*, **18**, 27102-27108 (2016).
35. Wei H., Xiao J., Yang Y., Lv S., Shi J., Xu X., Dong J., Luo Y., Li D., Meng Q.; Freestanding flexible carbon electrode for highly efficient hole-conductor-free perovskite solar cells, *Carbon*, **93**, 861-868 (2015).
36. Zhang F., Yang X., Wang H., Cheng M., Zhao J., Sun L.; Structure engineering of hole-conductor free perovskite-based solar cells with low-temperature processed commercial carbon paste as cathode, *ACS Appl. Mater. Interfaces*, **6**, 16140-16146 (2014).
37. Hu R., Chu L., Zhang J., Li X., Huang W.; Carbon materials for enhancing charge transport in the advancements of perovskite solar cells, *J. Power Sources*, **361**, 259-275 (2017).
38. Rong Y., Liu L., Mei A., Li X., Han H.; Beyond efficiency: the challenge of stability in mesoscopic perovskite solar cells, *Adv. Energy Mater.*, **5** (2015).
39. Hu Y., Si S., Mei A., Rong Y., Liu H., Li X., Han H.; Stable large-area ($10 \times 10 \text{ cm}^2$) printable mesoscopic perovskite module exceeding 10% efficiency, *Sol. RRL*, **1** (2017).
40. Jiang X., Yu Z., Lai J., Zhang Y., Hu M., Lei N., Wang D., Yang X., Sun L.; Interfacial engineering of perovskite solar cells by employing a hydrophobic copper phthalocyanine derivative as hole-transporting material with improved performance and stability, *Chem Sus Chem*, **10**, 1838-1845 (2017).
41. Priyadarshi A., Haur L.J., Murray P., Fu D., Kulkarni S., Xing G., Sum T.C., Mathews N., Mhaisalkar S.G.; A large area (70 cm^2) monolithic perovskite solar module with a high efficiency and stability, *Energy Environ. Sci.*, **9**, 3687-3692 (2016).

42. Rong Y., Hou X., Hu Y., Mei A., Liu L., Wang P., Han H., Synergy of ammonium chloride and moisture on perovskite crystallization for efficient printable mesoscopic solar cells, *Nat. Commun.*, **8** (2017).
43. Sheng Y., Hu Y., Mei A., Jiang P., Hou X., Duan M., Hong L., Guan Y., Rong Y., Xiong Y.; Enhanced electronic properties in $\text{CH}_3\text{NH}_3\text{PbI}_3$ via LiCl mixing for hole-conductor-free printable perovskite solar cells, *J. Mater. Chem. A*, **4**, 16731-16736 (2016).
44. Chen J., Xiong Y., Rong Y., Mei A., Sheng Y., Jiang P., Hu Y., Li X., Han H.; Solvent effect on the hole-conductor-free fully printable perovskite solar cells, *Nano Energy*, **27**, 130-137 (2016).
45. Chen H., Wei Z., He H., Zheng X., Wong K.S., Yang S.; Solvent engineering boosts the efficiency of paintable carbon-based perovskite solar cells to beyond 14%, *Adv. Energy Mater.*, **6**, 216-226 (2016).
46. Bai S., Cheng N., Yu Z., Liu P., Wang C., Zhao X.-Z.; Cubic: column composite structure $(\text{NH}_2\text{CH}=\text{NH}_2)_x(\text{CH}_3\text{NH}_3)^{1-x}\text{PbI}_3$ for efficient hole-transport material-free and insulation layer free perovskite solar cells with high stability, *Electrochim. Acta*, **190**, 775-779 (2016).
47. Liang J., Wang C., Wang Y., Xu Z., Lu Z., Ma Y., Zhu H., Hu Y., Xiao C., Yi X.; All inorganic perovskite solar cells, *J. Am. Chem. Soc.*, **138**, 15829-15832 (2016).
48. Li Z., Kulkarni S.A., Boix P.P., Shi E., Cao A., Fu K., Batabyal S.K., Zhang J., Xiong Q., Wong L.H.; Laminated carbon nanotube networks for metal electrode-free efficient perovskite solar cells, *ACS Nano*, **8**, 6797-6804 (2014).
49. Wei Z., Chen H., Yan K., Zheng X., Yang S.; Hysteresis-free multi-walled carbon nanotube-based perovskite solar cells with a high fill factor, *J. Mater. Chem. A*, **3**, 24226-24231 (2015).
50. Wang B., Liu T., Zhou Y., Chen X., Yuan X., Yang Y., Liu W., Wang J., Han H., Tang Y.; Hole-conductor-free perovskite solar cells with carbon counter electrodes based on ZnO nanorod arrays, *Phys. Chem. Chem. Phys.*, **18**, 27078-27082 (2016).
51. Cheng N., Liu P., Bai S., Yu Z., Liu W., Guo S.-S., Zhao X.-Z.; Application of mesoporous SiO_2 layer as an insulating layer in high performance hole transport material free $\text{CH}_3\text{NH}_3\text{PbI}_3$ perovskite solar cells, *J. Power Sources*, **321**, 71-75 (2016).
52. Zheng X., Chen H., Li Q., Yang Y., Wei Z., Bai Y., Qiu Y., Zhou D., Wong K.S., Yang S.; Boron doping of multiwalled carbon nanotubes significantly enhances hole extraction in carbon-based perovskite solar cells, *Nano Lett.*, **17**, 2496-2505 (2017).
53. Foresman, J.B. and Frisch, A.; Exploring Chemistry with Electronic Structure Methods, 2nd ed., Gaussian Inc., Pittsburgh, PA (1996).
54. Ibrahim M., Osman O.; Spectroscopic analyses of cellulose: Fourier transform infrared and molecular modelling study, *J. Comput. Theor. Nanosci.*, **6 (5)**, 1054-1058 (2009).
55. Ibrahim M.; Molecular modeling and FTIR study for K, Na, Ca and Mg coordination with organic acid, *J. Comput. Theor. Nanosci.*, **6 (3)**, 682-685(2009).
56. Youness R.A., Taha M.A., Ibrahim M.A.; Effect of Sintering Temperatures on the In Vitro Bioactivity, Molecular Structure and Mechanical Properties of Titanium/Carbonated Hydroxyapatite Nanobiocomposites, *J. Mol. Struct.*, **1150**, 188-195 (2017).
57. Abdelsalam H., Elhaes H., Ibrahim M.A.; First principles study of edge carboxylated graphene quantum dots, *Physica B*, **537**, 77-86 (2018).
58. Grenni P., Caracciolo A.B., Mariani L., Cardoni M., Riccucci C., Elhaes H., Ibrahim M.A.; Effectiveness of a new green technology for metal removal from contaminated water, *Microchem. J.*, **147**, 1010-1020 (2019).
59. Ibrahim M., Kholmurodov K.T., Fadeikina I.N., Morzhuhina S.V., EvgeniyaPopova S., Elhaes H., Mahmoud A-A; On the Molecular Modelling Structure of the Egyptian Soil/Sediment in River Nile Delta Region, *J. Comput. Theor. Nanosci.*, **14 (8)**, 4133-4136 (2017).
60. Abdelsalam H., Teleb N.H., Yahia I.S., Zahran H.Y., Elhaes H., Ibrahim M.A.; First principles study of the adsorption of hydrated heavy metals on graphene quantum dots, *J. Phys. Chem. Solids*, **130**, 32-40(2019).

61. Soler J.M., Artacho E., Gale J.D., García A., Junquera J., Ordejón P., Sánchez-Portal D.; The SIESTA method for ab initio order-N materials simulation, *J. Phys. Condens. Matter.*, **14**, 2745 (2002).
62. Klimesm J., Bowler D.R., Michaelides A.; Van der Waals density functionals applied to solids, *Phys. Rev. B*, **83**, 195131 (2011).
63. Giannozzi P., Baroni S., Bonini N., Calandra M., Car R., Cavazzoni C., Ceresoli D., Chiarotti G.L., Cococcioni M., Dabo I., Dal Corso A.; QUANTUM ESPRESSO: a modular and open-source software project for quantum simulations of materials, *J. Phys. Condens. Matter.*, **21**, 395502 (2009).
64. Saffari M., Mohebpour M.A., Soleimani H.R., Tagani M.B.; DFT analysis and FDTD simulation of $\text{CH}_3\text{NH}_3\text{PbI}_3\text{-xCl}_x$ mixed halide perovskite solar cells: role of halide mixing and light trapping technique, *J. Phys. D: Appl. Phys.*, **50** (41), 415501 (2017).
65. Even J., Pedesseau L., Jancu J.M., Katan C.; Importance of spin-orbit coupling in hybrid organic/inorganic perovskites for photovoltaic applications, *J. Phys. Chem. Lett.*, **4**, 2999-3005(2013).
66. Huang L.Y., Lambrecht W.R.; Electronic band structure, phonons, and exciton binding energies of halide perovskites CsSnCl_3 , CsSnBr_3 , and CsSnI_3 , *Phys. Rev. B*, **88**, 165203 (2013).
67. Mosconi E., Umari P., De Angelis F.; Electronic and optical properties of MAPbX_3 perovskites ($X = \text{I}, \text{Br}, \text{Cl}$): a unified DFT and GW theoretical analysis, *Phys. Chem. Chem. Phys.*, **18**, 27158-27164(2016).
68. Bokdam M., Sander T., Stroppa A., Picozzi S., Sarma D.D.; Franchini C., Kresse G.; Role of polar phonons in the photo excited state of metal halide perovskites, *Sci. Rep.*, **6**, 28618 (2016).
69. Tao S.X., Cao X., Bobbert P.A.; Accurate and efficient band gap predictions of metal halide perovskites using the DFT-1/2 method: GW accuracy with DFT expense, *Sci. Rep.* **7**, 14386 (2017).
70. Hernández-Haro N., Ortega-Castro J., Martynov Y.B., Nazmitdinov R.G., Frontera A.; DFT prediction of band gap in organic-inorganic metal halide perovskites: An exchange-correlation functional benchmark study, *Chem. Phys.*, **516**, 225-231(2019).
71. Yu C.J.; Advances in modelling and simulation of halide perovskites for solarcell applications, *J. Phys.: Energy*, **1**(2) 022001 (2019).
72. Lee M.M., Teuscher J., Miyasaka T., Murakami T.N., Snaith H.J.; Efficient Hybrid Solar Cells Based on Meso-Superstructured Organometal Halide Perovskites, *Science*, **338** (6107), 643-647(2012).
73. Snaith H.J.; Perovskites: the emergence of a new era for low-cost, high-efficiency solar cells, *J. Phys. Chem. Lett.*, **4**(21), 3623–3630(2013).

أفاق استخدام خلايا بيروفسكيت الشمسيّة القائمة على الكربون

فلاديسلاف كينيف¹, بافل جلاذيف¹ و مدحت ابراهيم²

¹جامعة دوبنا- دوبنا- روسيا الاتحادية.

²قسم الطيف- المركز القومى للبحوث - 33 شارع البحوث - 12622 الدقى- الجيزة- مصر.

عام 2009 تم لأول مره استخدام الخلايا الشمسية التي تعتمد على مواد البيرفسكيت في تكوينها. ومنذ ذلك الحين أصبحت مواد البيرفسكيت من المواد المهمه التي تدخل في تركيب الخلايا الشمسية نظر لكتاء امتصاص الضوء التي تنتفع بها. وزادت اهميه هذا النوع من المواد في الخلايا الشمسية بعد استخدام طريقة الترسيب الكيميائي ذاتي الاصنادي في التحضير. كما تم مؤخرا تحضير مزيج مهجن من بيرفسكيت يحتوي على مواد عضوية وغير عضوية مثل

Organic-inorganic hybrid lead-halide perovskite solar cells (PSCs)
استخدمت كخلايا شمسية بكفاءة بلغت حوالي 23.7%. والجدير بالذكر ان هناك محاولات تطوير مستمرة في هذا المجال لنقليل التكلفة وذلك باستخدام خلايا شمسية من النوع

Carbon-based hole-conductor-free perovskite solar cells (CPSCs)
والغرض هو الحصول على درجة ثبات اعلى وتكلفه اقل في مجال استخدام مواد البيرفسكيت في تحضير الخلايا الشمسية.